# Crustal stress patterns: Analysis of *Ps* splitting for seismic anisotropy

**Abhishek Rai[1,*], S. S. Rai[2] and V. K. Gaur[3]**

[1]National Centre of Experimental Mineralogy and Petrology, University of Allahabad, Allahabad 211 002, India
[2]National Geophysical Research Institute, Hyderabad 500 007, India
[3]Indian Institute of Astrophysics, Bangalore 560 0 034, India

**Broadband seismograms from seismic stations located on various geologic terranes of the south Indian shield, were analysed to determine the anisotropy characteristics of the underlying crust: orientation of the axes of symmetry and the degree of anisotropy. Analysis of the split measured in the deconvolved radial and transverse *P*-to-*S* converted components from the Moho indicates that the anisotropic axis lies approximately E–W in the high-grade Granulite stations and almost N–S in the adjoining low-grade Dharwar Craton, with an average split-time of about 0.34 ± 0.10 s. Observed directions of the vertically averaged anisotropy are in reasonably good agreement with the geologic expressions of the region, though not necessarily conforming with the plate velocity, indicating that their sources lie in the stress/strain fields accumulated in the crust.**

**Keywords:** Crustal anisotropy, Indian shield, receiver functions.

THE south Indian shield is comprised of a variety of metamorphic rocks (Figure 1). These range from the low-grade granite greenstones (3.4 Ga) of the Dharwar Craton that transit southward into the 2.5 Ga high-grade granulites and charnockites, to the Pan-African granulites and khondalites (of meta-sedimentary origin) further south. The eastern margin of the Dharwar Craton is fringed by another narrow belt of granulites that forms the eastern passive continental margin of the Indian Peninsula[1,2]. This study was aimed at investigating the seismic anisotropy in the crust of the south Indian shield with the objective of gaining an understanding of the stress regime accumulated in the crust.

Laboratory experiments[3] and petrophysical studies[4–6] suggest that most of the rocks comprising the earth's crust are anisotropic to some degree, their major sources being preferred orientation of minerals, small-scale compositional layering and oriented system of cracks, microcracks and fractures[3,7,8]. Close association of contemporary crustal strains to cracks and fractures resulted in the hypothesis of 'extensive dilatancy anisotropy' (EDA)[9], arising from fine layering[10], aligned cracks and preferentially oriented pore spaces[3,8] which may induce ~5–12% anisotropy in the crust[11,12].

*For correspondence. (e-mail: akr_ncemp@yahoo.co.in)

Observations[13] also show that the directions of the largest and smallest shear-wave velocities in the crust coincide remarkably well with the largest and smallest horizontal tectonic stress directions respectively. Therefore, crustal anisotropy can be regarded as an indicator of the crustal stress/strain regime, besides serving to separate the contributions from the upper mantle anisotropy appearing in SKS (shear-waves generated at the core–mantle boundary) splittings, which may otherwise lead to a misplaced interpretation of the upper mantle dynamics. Fortunately, crustal anisotropy can be determined directly from the Moho-converted shear phases splittings[14], and this approach has been used to study the anisotropic character of the various crustal elements that constitute the south Indian shield, by analysing the splittings of the Moho-converted shear phases observed on deconvolved radial and transverse components of broadband seismograms recorded at stations located in the shield.

Receiver functions are time series extracted from three component (N–S, E–W and *Z*-components) seismograms, representing the converted phases from various seismic discontinuities in the subsurface. Among these, the Moho-converted shear phases are the most prominent and therefore easily identified on radial–transverse components of the receiver functions. The *P*-to-*S* converted phases and their reverberations recorded on the horizontal components

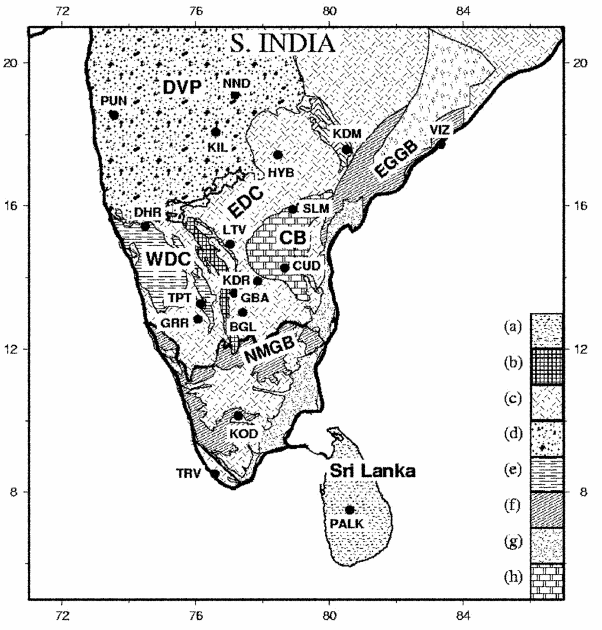


**Figure 1.** Geological map of the south Indian shield. (a) Sri Lanka Granulite terrane, (b) Closepet granite, (c) Peninsular gneisses, (d) Deccan Volcanic Province (DVP), (e) Western Dharwar schists (WDC), (f) Granulites and charnockites, (g) Gondwana sediments and (h) Proterozoic sediments of the Cuddapah Basin (CB). NMGB, Nilgiri Madurai Granulite Belt; EGGB, Eastern Ghats Granulite Belt.

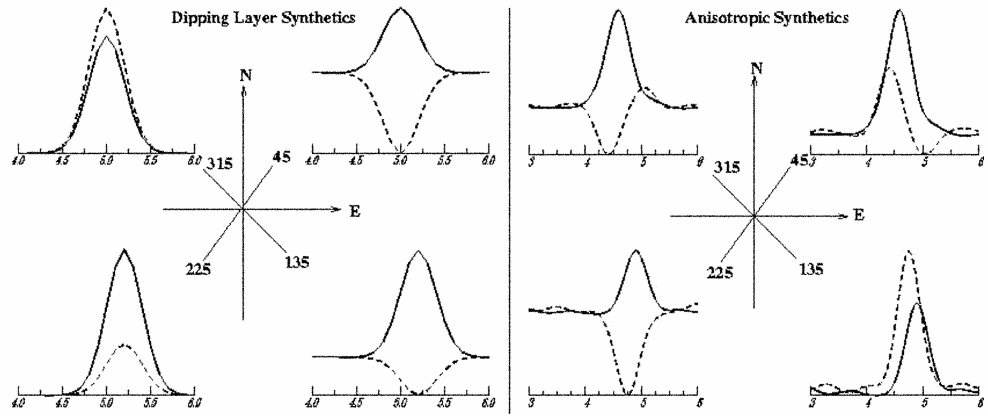


**Figure 2.** Examples of synthetic receiver function for dipping layers and anisotropy in the subsurface (radial, solid line and transverse, dashed line). No split was observed for dipping layer synthetics, except polarity reversal, while clear split was obvious on anisotropic synthetics besides polarity reversals.

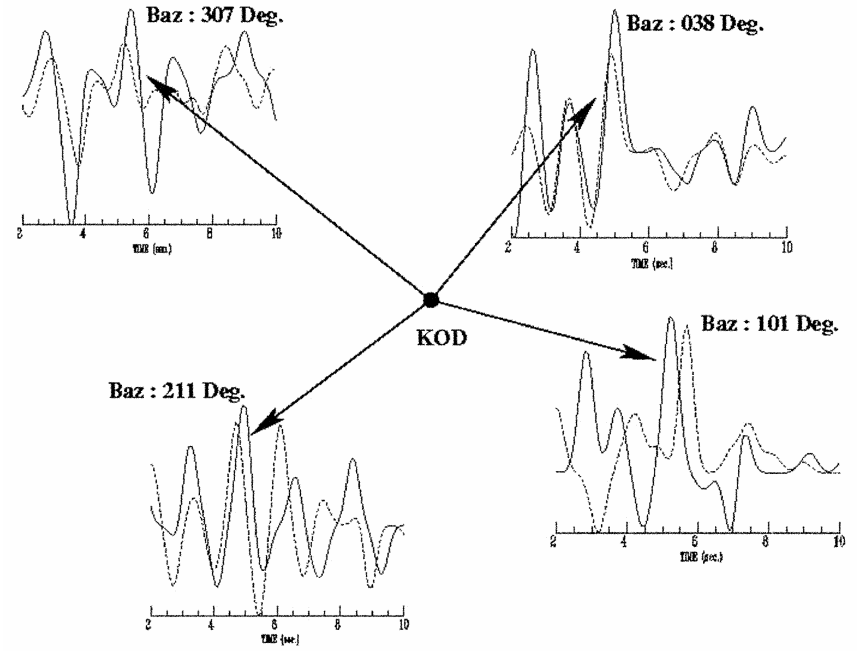


**Figure 3.** Radial (solid lines) and transverse (dashed lines) receiver functions for Kodaikanal (KOD; corrected for polarity reversal) superposed on each other. Moho-converted arrivals are indicated by arrows. Arrivals from various azimuths clearly indicate split.

can be isolated from the source signature and more distant propagation effects, by deconvolving the vertical component of the seismogram from the radial and transverse components. The resulting radial component time series closely corresponds to the impulse response of the earth structure beneath a seismic receiver and is called the radial receiver function[15]. The corresponding transverse component time series which should be zero for an ideal homogeneous, isotropic, horizontally-stratified crust, provides a measure of the deviation of the underlying crustal structure from these ideal conditions. Since these phases originate at the crust–mantle boundary, they contain integrated contribution of the entire crust, thereby representing the vertically averaged seismic anisotropy in the crust.

While several methods have been used for deconvolving the vertical from the horizontal component time series[15–19], the iterative deconvolution technique[18] has been used in this study because it provided the most stable receiver functions for the seismogram records from the area under

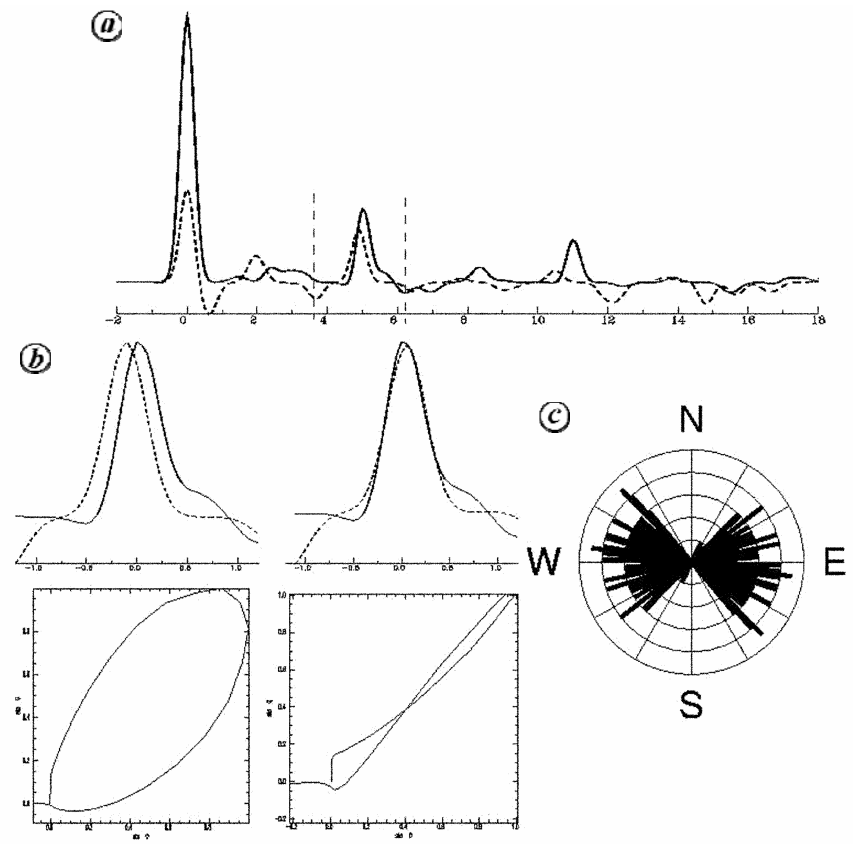


**Figure 4.** Example showing analysis of splitting of Moho-converted *Ps* phase recorded on receiver functions. ***a***, Radial (solid line) and transverse (dashed line) receiver functions. The analysis window is shown by vertical lines around the Moho-converted *Ps* phase. ***b***, The analysis window and the corresponding particle motion plots, before and after analysis. Linear motion indicates that the splitting effect has been successfully removed by the cross-correlation technique. ***c***, The azimuth of vertically averaged anisotropy, after a similar kind of analysis on a number of receiver functions.

this study. This method assumes that the radial seismogram is a convolution of the vertical component with the earth structure, so that the latter can be isolated by extracting a time series which, when convolved with the vertical component, would approximate the horizontal component. This is accomplished by a least-square minimization of the difference between the observed horizontal seismogram and a predicted signal generated by the convolution of an iteratively updated spike train with the vertical. This procedure renders the resulting receiver functions relatively free from any deconvolution-induced noise such as those observed in the water-level deconvolution technique[16].

Teleseismic records from seismic stations installed over a variety of geological terranes of the south Indian shield[20] constituted the data for this study. Receiver functions were calculated for all high signal-to-noise ratio seismograms of events with magnitudes greater than 5.5, lying within the epicentral distance range 30–90°. Considering only the teleseismic records in this study ensures that the seismograms are almost free from the far-field scattered energy[21]. Finally, only seismograms which show polarization anomalies[22,23] less than ±5° were considered for further analysis. They were low-pass filtered with a Gaussian of 3.5, thereby eliminating frequencies greater than ~1.7 Hz. RFs with clear presence of Moho-converted *Ps* phases on both the components were selected for further analysis.

Synthetic tests (Figure 2) indicate that dipping layers in the subsurface or presence of seismic anisotropy could deviate large energy from radial to transverse component along with phase reversals. However, splitting of the *Ps* phases recorded on radial–transverse pair is uniquely observed only if anisotropy is present in the subsurface. Before analysing the splitting, transverse receiver functions with inverted polarity of the Moho-converted *Ps* phase were corrected for polarity reversal. Radial (solid) and transverse (dotted) receiver functions, superimposed on each other, for a seismic station installed on the South Indian high-grade granulite terrane (Kodaikanal, KOD) are shown in Figures 3 and 4. Percentage and orientation of the vertically averaged seismic anisotropy in the crust, were then determined by the cross-correlation technique[12,14,24,25]. This technique exploits the fact that in the

**Table 1.** Summary of azimuth of anisotropy ($\phi$) and split time ($\delta t$) derived by analysing the Moho converted *Ps* phases

| Station | Latitude, longitude (deg.) | No. of events | $\phi$ (deg. from *N*) | $\delta t$ (s) |
|---|---|---|---|---|
| Bangalore (BGL) | 77.57, 13.02 | 069 | –02.9 ± 25.6 | 0.29 ± 0.12 |
| Cuddapah (CUD) | 78.76, 14.47 | 037 | –63.0 ± 21.1 | 0.28 ± 0.10 |
| Dharwar (DHR) | 74.98, 15.43 | 015 | –12.3 ± 17.6 | 0.37 ± 0.09 |
| Gauribidnaur (GBA) | 77.35, 13.56 | 065 | –13.0 ± 24.8 | 0.31 ± 0.12 |
| Gorur (GRR) | 76.06, 12.83 | 070 | 00.0 ± 25.0 | 0.38 ± 0.12 |
| Hyderabad (HYB) | 78.55, 17.42 | 051 | –27.7 ± 32.0 | 0.40 ± 0.10 |
| Kadiri (KDR) | 78.16, 14.17 | 014 | –07.0 ± 25.0 | 0.34 ± 0.11 |
| Kodad (KDM) | 80.65, 17.57 | 024 | –0.6 ± 19.3 | 0.39 ± 0.08 |
| Killari (KIL) | 76.59, 18.06 | 057 | –00.7 ± 23.1 | 0.33 ± 0.14 |
| Kodaikanal (KOD) | 77.46, 10.23 | 067 | –64.8 ± 21.9 | 0.27 ± 0.08 |
| Lattavaram (LTV) | 77.28, 14.93 | 031 | –02.2 ± 23.9 | 0.33 ± 0.13 |
| Nander (NND) | 77.28, 19.11 | 053 | –01.8 ± 22.4 | 0.35 ± 0.12 |
| Pallekele (PALK) | 80.70, 07.27 | 031 | –62.8 ± 16.1 | 0.28 ± 0.10 |
| Pune (PUN) | 73.85, 18.53 | 016 | –11.0 ± 22.6 | 0.36 ± 0.13 |
| Srisailam (SLM) | 78.89, 16.10 | 053 | –60.0 ± 19.5 | 0.35 ± 0.10 |
| Tiptur (TPT) | 76.54, 13.27 | 047 | –1.6 ± 15.6 | 0.38 ± 0.11 |
| Thiruvananthapuram (TRV) | 76.96, 08.51 | 026 | –64.9 ± 16.6 | 0.42 ± 0.11 |
| Vishakhapatnam (VIZ) | 83.33, 17.72 | 020 | 30.3 ± 22.5 | 0.32 ± 0.10 |

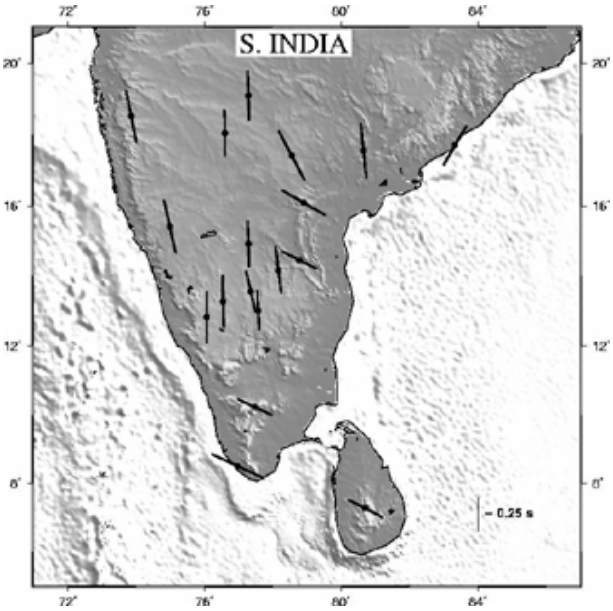


**Figure 5.** Average azimuths and split times of vertically averaged crustal anisotropy at the South Indian and Sri Lankan stations. Stations located on the southern Granulite terrane show an almost E–W direction for crustal anisotropy, while the dominant direction of the azimuth of crustal anisotropy for stations on the Dharwar craton is directed almost along N–S. The line lengths correspond to split times.

fast–slow coordinate system, the components of the split *Ps* phase are expected to be almost similar since they are generated by the same parent phase. This was achieved by incrementally rotating the two orthogonal components of receiver functions from –90° to 90° in steps of 1° at a time, and their cross-correlation coefficients calculated for time lags of –0.5 to +0.5 s in steps of 0.01 s. The rotation angle and the time-step required for obtaining the maximum cross-correlation coefficient yielded the azimuth and strength of the averaged vertical anisotropy in the crust. The time lags and the azimuth between the split Moho-converted *Ps* phases provide a measure of the percentage of anisotropy present in the subsurface and its orientation. These quantities were determined for each of the Indian shield stations to study their shared and distinctive anisotropic characteristics. These are discussed below.

Table 1 and Figure 5 present a summary of the split parameters obtained for various stations of the Indian shield. Orientation of the anisotropy axis, yielded by this analysis, is found to be approximately East–West for stations located on the southern high-grade Granulite terranes of India and Sri Lanka (KOD, TRV and PALK), with an average split of $0.32 \pm 0.10$ s and azimuth of $-64.16 \pm 13.16°$ from north. These directions correlate rather well with the dominantly E–W-directed geological fabric of these terranes[1,26]. Stations located on the Proterozoic Cuddapah basin (SLM and CUD) also show a similar trend. However, the inherent cause of anisotropy for these two terranes of the Indian shield, i.e. south Indian Granulite terrane and Cuddapah basin, may be different and related to their origin, which is undoubtedly different[1]. For most of the other stations on the eastern and western Dharwar Craton along with those on the Deccan volcanic province, the symmetry axis is found to be oriented almost along N–S (Table 1 and Figure 5), which also correlates well with the well-documented pervasive north–south grains of the major geological features of the craton[1]. The Dharwar craton data, which indicate a N–S alignment for the azimuth of anisotropy are also consistent with the stress pattern derived through the study of bore-hole

breakouts and hydraulic fracturing stress measurements[27], as well as observations of the geologic fabric[1] developed by prevailing tectonic forces working in the region.

Assuming that crustal anisotropy is uniformly distributed in whole of the crust and a mean crustal thickness of about 40 km, ~2% anisotropy may be assigned to both the Dharwar craton and the Granulite terranes. However, good correlation of the azimuth of anisotropy with the structural grains of these terranes which are expected to fade at depth, suggests that most of the inferred anisotropy is confined to the upper-most few kilometres of the crust or at least the upper crustal anisotropy has a dominant effect on the type of analysis performed in this study. Assuming that all of the anisotropy is confined in the upper crust up to a depth of 15 km, the degree of anisotropy would be ~5–6%. Modelling of stress due to topography and density inhomogeneities shows that stresses in the crust are largely concentrated in the upper 15 km, which could produce EDA cracks and fractures causing about 5–10% seismic anisotropy in the crust[28]. These, in all likelihood, also constitute the primary source of crustal anisotropy inferred for the Indian shield.


1. Naqvi, S. M. and Rogers, J. J. W., *Precambrian Geology of India*, Oxford Univ. Press, Oxford, 1987.
2. Raith, M., Karmakar, S. and Brown, M., Ultra-high-temperature metamorphism and multi-stage decompressional of saphirrine granulites from the Palni-Hill ranges, southern India. *J. Metamorphic Geol.*, 1997, **15**, 379–399.
3. Babuska, V. and Cara, M., *Seismic Anisotropy in the Earth*, Kluwer Academic Press, Amsterdam, 1991.
4. Barruol, G. and Mainprice, D., A quantitative evaluation of the contribution of crustal rocks to the shear wave splitting of teleseismic SKS waves. *Phys. Earth Planet. Inter*., 1993, **78**, 281–300.
5. Alsina, D. and Snieder, R., Small-scale sublithospheric continental mantle deformation: Constraints from SKS splitting observations. *Geophys. J. Int.*, 1995, **123**, 431–448.
6. Weiss, T., Siegesmund, S., Rabbel, W., Bohlen, T. and Pohl, M., Seismic velocities and anisotropy of the lower continental crust. *Pure Appl. Geophys*., 1999, **156**, 97–122.
7. Leary, P., Crampin, S. and McEvilly, T., Seismic fracture anisotropy in the earth's crust: An overview. *J. Geophys. Res*., 1990, **95**, 11105–11114.
8. Crampin, S., The fracture criticality of crustal rocks. *Geophys. J. Int*., 1994, **118**, 428–438.
9. Crampin, S., Earthquake prediction: A new physical basis. *Geophys. J. R. Astron. Soc*., 1984, **76**, 147–156.
10. Backus, G., Long-wave elastic anisotropy produced by horizontal layering. *J. Geophys. Res*., 1962, **67**, 4427–4440.
11. Vergne, J., Wittlinger, G., Farra, V. and Su, H., Evidence for upper crustal anisotropy in the Songpan-Ganze northern Tibet terrane. *Geophys. Res. Lett*., 2003, **30**, 1552–1556.
12. Bowman, J. R. and Ando, M., Shear-wave splitting in the upper-mantle wedge above the Tonga subduction zone. *Geophys. J. R. Astron. Soc*., 1987, **88**, 25–41.
13. Turchaninov, I., Panin, V., Markov, G., Pavlovskii, V., Sharov, N. and Ivanov, G., On correlation between seismic velocity anisotropy and stresses *in situ*. *Pageoph*, 1977, **115**, 259–265.
14. McNamara, D. E. and Owens, T. J., Azimuthal shear wave velocity anisotropy in the Basin and Range Province using Moho Ps converted phases. *J. Geophys. Res*., 1993, **98**, 12003–12017.
15. Langston, C.A., Structure under Mt. Ranier, Washington, inferred from teleseismic body waves. *J. Geophys. Res.*, 1979, **84**, 4749–4762.
16. Ammon, C. J., The isolation of receiver effects from teleseismic *P*-waveforms. *Bull. Seismol. Soc. Am.*, 1991, **81**, 2504–2510.
17. Gurrola, H., Baker, G. E. and Minster, J. B., Simultaneous time-domain deconvolution with application to the computation of receiver function. *Geophys. J. Int*., 1995, **120**, 537–543.
18. Ligorria, J. P. and Ammon, C. J., Iterative deconvolution and receiver–function estimation. *Bull. Seismol. Soc. Am*., 1999, **89**, 1395–1400.
19. Park, J. and Levin, V., Receiver functions from multi-taper spectral correlation estimates. *Bull. Seismol. Soc. Am.*, 2000, **90**, 1507–1520.
20. Rai, S. S., Priestley, K. P., Suryaprakasham, K., Srinagesh, D., Gaur, V. K. and Du, Z., Crustal shear velocity structure of the south (Indian) shield. *J. Geophys. Res*., 2003, **108**, 2088–2099.
21. Nolet, G. and Dahlen, F., Wave front healing and the evolution of seismic delay times. *J. Geophys. Res*., 2000, **105**, 19043–19054.
22. Kanasewich, E. R., *Time Sequence Analysis in Geophysics*, The University of Alberta Press, 1975.
23. Jurkevics, A., Polarization analysis of three-component array data. *Bull. Seismol. Soc. Am*., 1988, **78**, 1725–1743.
24. Herquel, G., Wittlinger, G. and Guilbert, J., Anisotropy and crustal thickness of northern Tibet: New constraints for tectonic modeling. *Geophys. Res. Lett*., 1995, **22**, 1925–1928.
25. Tong, C., Gudmundsson, O. and Kennett, B., Shear wave splitting in refracted waves returned from the upper mantle transition zone beneath northern Australia. *J. Geophys. Res.*, 1994, **99**, 15783–15797.
26. Mukhopadhyay, D., Senthil Kumar, P., Srinivasan, R. and Bhattacharya, T., Nature of Palghat–Cauvery Lineament in the region south of Namakkal, Tamil Nadu: Implications for terrane assembly in south Indian Granulite Province. *Mem. Geol. Soc. India*, 2003, **50**, 279–296.
27. Gowd, T., Rao, S. and Gaur, V. K., Tectonic stress field in the subcontinent. *J. Geophys. Res*., 1992, **97**, 11879–11888.
28. Mandal, P. and Singh, R., Three-dimensional intraplate stress distributions associated with topography and crustal density inhomogeneities beneath the Deccan Volcanic Province. *Proc. Indian Acad. Sci*. (*Earth Planet. Sci*.), 1996, **105**, 143–153.


ACKNOWLEDGEMENTS. A.R. thanks the Cambridge Commonwealth Trust for providing scholarship to do a Ph D at the University of Cambridge where a part of this work was completed. We thank the India Meteorological Department for providing data from stations of their seismic network and the Department of Science and Technology, New Delhi for financial support under the deep continental studies programme. We also thank Keith Priestley, and Alok K. Gupta for their valuable suggestions during this study.

Received 8 May 2007; revised accepted 29 January 2008